

Characterization of Negative Allosteric Modulators of the Calcium-Sensing Receptor for Repurposing as a Treatment of Asthma[§]

Polina L. Yarova, Ping Huang, Martin W. Schepelmann, Richard Bruce, Rupert Ecker, Robert Nica, Vsevolod Telezhkin, Daniela Traini, Larissa Gomes dos Reis, Emma J. Kidd, William R. Ford, Kenneth J. Broadley, Benson M. Kariuki, Christopher J. Corrigan, Jeremy P.T. Ward, Paul J. Kemp, and Daniela Riccardi

Schools of Biosciences (P.L.Y., P.H., M.W.S., R.B., P.J.K., D.R.), Pharmacy (E.J.K., W.R.F., K.J.B.), and Chemistry (B.M.K.), Cardiff University, Cardiff, United Kingdom; Institute for Pathophysiology and Allergy Research, Medical University of Vienna, Vienna, Austria (M.W.S.); TissueGnostics GmbH, Vienna, Austria (R.E., R.N.); School of Dental Sciences, University of Newcastle, United Kingdom (V.T.); Woolcock Institute of Medical Research, The University of Sydney, Sydney, Australia (D.T., L.G.d.R.); and School of Immunology & Microbial Sciences, King's College London, London, United Kingdom (C.J.C., J.P.T.W.)

Received August 8, 2020; accepted October 5, 2020

ABSTRACT

Asthma is still an incurable disease, and there is a recognized need for novel small-molecule therapies for people with asthma, especially those poorly controlled by current treatments. We previously demonstrated that calcium-sensing receptor (CaSR) negative allosteric modulators (NAMs), calcilytics, uniquely suppress both airway hyperresponsiveness (AHR) and inflammation in human cells and murine asthma surrogates. Here we assess the feasibility of repurposing four CaSR NAMs, which were originally developed for oral therapy for osteoporosis and previously tested in the clinic as a novel, single, and comprehensive topical antiasthma therapy. We address the hypotheses, using murine asthma surrogates, that topically delivered CaSR NAMs 1) abolish AHR; 2) are unlikely to cause unwanted systemic effects; 3) are suitable for topical application; and 4) inhibit airway inflammation to the same degree as the current standard of care, inhaled corticosteroids, and, furthermore, inhibit airway remodeling. All four CaSR NAMs inhibited poly-L-arginine-induced AHR in naïve mice and suppressed both AHR and airway inflammation in a murine surrogate of acute asthma, confirming class specificity. Repeated exposure to inhaled CaSR NAMs did not alter blood pressure, heart rate, or

serum calcium concentrations. Optimal candidates for repurposing were identified based on anti-AHR/inflammatory activities, pharmacokinetics/pharmacodynamics, formulation, and micronization studies. Whereas both inhaled CaSR NAMs and inhaled corticosteroids reduced airways inflammation, only the former prevented goblet cell hyperplasia in a chronic asthma model. We conclude that inhaled CaSR NAMs are likely a single, safe, and effective topical therapy for human asthma, abolishing AHR, suppressing airways inflammation, and abrogating some features of airway remodeling.

SIGNIFICANCE STATEMENT

Calcium-sensing receptor (CaSR) negative allosteric modulators (NAMs) reduce airway smooth muscle hyperresponsiveness, reverse airway inflammation as efficiently as topical corticosteroids, and suppress airway remodeling in asthma surrogates. CaSR NAMs, which were initially developed for oral therapy of osteoporosis proved inefficacious for this indication despite being safe and well tolerated. Here we show that structurally unrelated CaSR NAMs are suitable for inhaled delivery and represent a one-stop, steroid-free approach to asthma control and prophylaxis.

Introduction

More than 300 million people suffer from asthma worldwide with a substantial burden of morbidity and mortality (The Global Asthma Report, 2018). The current mainstay therapies

of inhaled corticosteroids (ICSs) and bronchodilators control symptoms resulting from airway obstruction reasonably well in most patients but may not be as effective at altering the natural history of airway obstruction and remodeling (An et al., 2007; O'Byrne et al., 2019). As a consequence, severe, therapy-resistant obstruction develops in a significant minority of patients, resulting in life-long impairment of quality of life, increased risk of hospital admission, and death (Hansbro et al., 2017). Furthermore, no current antiasthma drug *directly* targets bronchial smooth muscle hyperresponsiveness, a critical contributor to airway obstruction and the fundamental physiologic

This work was supported by King's College Commercialization Institute [Grant 510798], Marie Curie "Multifaceted calcium-sensing receptor (CaSR)" Education and Training Network (ETN) [Grant 264663], and CaSR Biomedicine [Grant 675228].

<https://doi.org/10.1124/jpet.120.000281>.

[§] This article has supplemental material available at jpet.aspetjournals.org.

ABBREVIATIONS: ACh, acetylcholine; AHR, airway hyperresponsiveness; BALF, bronchoalveolar lavage fluid; CaSR, calcium-sensing receptor; EtOH, ethanol; FP, fluticasone propionate; HEK, human embryonic kidney; IC₈₀, 80% inhibitory concentration; ICS, inhaled corticosteroid; L_{Ca}, L-type Ca²⁺; MCh, methacholine; NAM, negative allosteric modulator; OVA, ovalbumin; PD, pharmacodynamics; Penh, enhanced pause; PG, propylene glycol; PK, pharmacokinetics; PLA, poly-L-arginine.

abnormality characterizing asthma (Sterk and Bel, 1989; An et al., 2007). Therapies based on monoclonal antibodies (biologicals) targeting IgE binding or asthma-related cytokines reduce obstruction and exacerbations to an unpredictable extent in some but not all patients and are further limited by administration logistics and cost (Walsh, 2017). Consequently, there is a strong need for the development of novel small-molecule drugs that are preferably delivered topically using commercially available devices and target both bronchial smooth muscle hyperresponsiveness and airway inflammation.

The calcium-sensing receptor (CaSR) is a G protein-coupled receptor originally identified as the master controller for serum-ionized calcium levels (Brown et al., 1993). It is a multimodal receptor activated not only by divalent cations (Ca^{2+} , Mg^{2+}) but also by polycations released by cells involved in asthmatic airway inflammation, such as spermine, spermidine, and eosinophil-derived cationic proteins (Kurosawa et al., 1992; Maarsingh et al., 2008; Yarova et al., 2015). The CaSR is expressed in multiple tissues, including airway smooth muscle and inflammatory cells, and has been implicated in numerous cellular activities and several disorders independently of calcium homeostasis (Riccardi and Kemp, 2012; Yarova et al., 2015; Brennan et al., 2016; Hannan et al., 2018). Notably, the CaSR is an important regulator of inflammation via activation of the NLRP3 inflammasome (Lee et al., 2012; Rossol et al., 2012). Using murine asthma surrogates and cultured human asthmatic smooth muscle cells, we have recently presented evidence consistent with the hypothesis that airway hyperresponsiveness (AHR) in human asthma reflects abnormal expression of the CaSR and shown that small-molecule CaSR negative allosteric modulators (NAMs), also known as calcilytics, abolish both AHR and airway inflammation (Yarova et al., 2015; Corrigan, 2020).

We have previously used commercially available CaSR NAMs as pharmacological tools, but their limited bioavailability detracts from their suitability for clinical development (Yarova et al., 2015). However, several pharmaceutical companies have developed and assessed (up to phase 2 clinical trials) systemically delivered CaSR NAMs for efficacy in reversing osteoporosis, namely the amino alcohols NPSP-795, Ronacaleret, and JTT-305 and the quinazolin-2-one AXT-914 (Kumar et al., 2010; Caltabiano et al., 2013; Halse et al., 2014; John et al., 2014). Although they exhibited good safety and tolerability profiles, they were found not to be efficacious for postmenopausal osteoporosis and induced hypercalcemia in some patients; their further development for treating osteoporosis was therefore halted (Nemeth et al., 2018). Since CaSR NAMs have the potential advantage of suppressing both AHR and inflammation, in this investigation we address the hypothesis that these four clinically tested CaSR NAMs can be repurposed as a novel, single-drug, topical antiasthma therapy that will obviate the need for both topical bronchodilator and corticosteroid therapy. To achieve this, we aimed to characterize, in terms of pharmacology, safety, efficacy, pharmacokinetics (PK)/pharmacodynamics (PD), and lack of systemic effects as well as the suitability of existing calcilytics for topical therapy of human asthma and to compare their effects with those of the current standard of care, topical ICS, in a chronic murine model of Th2/IgE-driven asthma.

Methods

In Vitro Studies

Determination of CaSR NAM Efficacies and Potencies In Vitro. All chemicals and reagents were obtained from Sigma-Aldrich, UK, unless otherwise specified. Human embryonic kidney (HEK) 293 cells stably expressing human CaSR (Ward et al., 2013) were loaded with the Ca^{2+} indicator fura-2 acetoxyethyl ester, and calcium imaging was carried out as previously described (Yarova et al., 2015) using an inverted microscope (IX71; Olympus) and fluorescence source (Xenon lamp). Extracellular solution contained (in millimolar) 135 NaCl, 5 KCl, 5 *N*-2-hydroxyethylpiperazine-*N'*-2-ethanesulfonic acid, 10 glucose, 1.2 MgCl_2 , and 0.5 CaCl_2 (pH = 7.4). A rapid perfusion system was used to alter extracellular Ca^{2+} concentration and apply test compounds.

Patch-Clamp Recordings of the Effects of CaSR NAMs on the L-Type Ca^{2+} Channels. Some CaSR NAMs are structural derivatives of dihydropyridines, compounds that affect the current via L-type Ca^{2+} channel. To examine whether CaSR NAMs had any effect on these channels, voltage and current recordings were made using conventional patch clamp in the whole-cell configuration in HEK293 cells stably expressing the $\alpha 1c$ subunit of L-type Ca^{2+} channels (CaV1.2) (Fearon et al., 2000) employing an Axopatch 200B amplifier interfaced to a computer running pClamp 9 using a Digidata 1322A A/D interface (Molecular Devices, Sunnyvale, CA). Recordings were digitized at 10 kHz and low-pass filtered at 2 or 5 kHz using an 8-pole Bessel filter. The bath solution for measurements of Ca^{2+} current contained (in millimolar) 95 NaCl, 5 CsCl, 0.6 MgCl_2 , 20 BaCl_2 , 10 HEPES, 15 D-glucose, and 20 tetraethylammonium chloride; pH was adjusted to 7.4 by 1 M NaOH. The standard pipette solution for Ca^{2+} current contained (in millimolar) 120 CsCl, 20 TEA, 2 MgCl_2 , 10 ethylene-glycol-tetra-acetic acid, 10 HEPES, 2 $\text{Na}_2\text{-ATP}$, and 1.6 Na-GTP; pH was adjusted to 7.2 with CsOH. For episodic stimulation, the following voltage-clamp protocol was used: holding potential -70 mV and 450-millisecond steps to 0 mV with 5-second time interval. Cell capacitance and series resistance were measured and compensated at between 60% and 90%. Tested compounds were introduced through the continuous flow system. Pipette resistances were 8–10 M Ω when filled with the pipette solutions. Data were analyzed using Clampfit 10.2.

Animal Studies

Animal Procedures. All animal procedures conformed to the regulations of the Animals (Scientific Procedures) Act 1986 and Declaration of Helsinki conventions for the use and care of animals and were approved by the Home Office (UK) and local ethics committee. Two- to three-month-old BALB/c mice were obtained from Envigo (UK), maintained under standard conditions with food and water ad libitum, and used in experiments at 6–8 weeks of age. According to the a priori F test power calculations for one-way omnibus ANOVA with α error probability of 0.05, power 0.8, and effect size 0.7, six mice were needed for each treatment group of the five groups per each experiment (30 animals in total per experiment; G*Power v.1.3.9.6). Male mice were used in all experiments with the exception of the in vivo head-to-head comparison of CaSR NAM with ICS. For these experiments only, in which inflammation was measured as the primary readout, female mice were used, owing to the heightened inflammatory response compared with male mice (Melgert et al., 2005; Blacquièrre et al., 2010). Animals were assigned at random to experimental groups, and in vivo and in vitro data were measured and analyzed by operators blinded to the experimental conditions.

Ex Vivo Measurements of Airway Reactivity. After humane euthanasia by a schedule 1 method (intraperitoneal pentobarbital overdose), tracheae were isolated from the mice and cleaned as previously described (Donovan et al., 2013). Each tracheal ring of 2 mm in length was then mounted into jaws of a small vessel wire myograph (DMT 610; Danish Myo Technology, Denmark) using steel

wires and left to equilibrate at 37°C in 5% CO₂/95% O₂-bubbled Krebs' buffer containing 2 mM Ca²⁺ to mimic proinflammatory conditions (118 mM NaCl, 3.4 mM KCl, 1.2 mM MgSO₄, 1.2 mM KH₂PO₄, 25 mM NaHCO₃, 2 mM CaCl₂, 11 mM glucose) for 20 minutes, after which the tracheal rings were gradually stretched to 5 mN, washed, and left to equilibrate for another 20 minutes. Parallel experiments were also carried out in Krebs' solution containing 1 mM Ca²⁺ to mimic physiologic conditions. Tracheae were then tested for viability with high K⁺ (40 and 80 mM), and acetylcholine (ACh) concentration-response curves were generated by cumulative addition of ACh to the bath. Preparations were then washed with Krebs' buffer before being half-maximally contracted with ACh at its EC₅₀ (10–30 nM). Cumulative concentration-response curves were then obtained for the CaSR NAMs and vehicle control (DMSO in Krebs' buffer).

Drug Nebulization. NPSP-795, Ronacaleret, JTT-305, and AXT-914 were custom-synthesized by Sygnature Discovery (BioCity, Nottingham, United Kingdom), whereas NPS2143 [positive control (Yarova et al., 2015)] was obtained from Tocris Bioscience (Bristol, United Kingdom). Compounds were delivered into a Perspex chamber using a SideStream nebulizer (Philips Respironics, Philips Hospital & Health Care, Amsterdam) equipped with a compressor (PulmoStar; Sunrise Medical, West Midlands, United Kingdom). Dosage estimation was carried out as described in the Supplemental Materials.

Measurements of Airway Obstruction. Measurements of airway obstruction were carried out using noninvasive barometric plethysmography (Buxco Research Systems, St. Paul, MN) in unrestrained, conscious mice as previously described (Fernandez-Rodriguez et al., 2010; Yarova et al., 2015), wherein enhanced pause (Penh) was used as an indicator of airway obstruction to study AHR, as previously described (Hamelmann et al., 1997; Yarova et al., 2015). Briefly, after establishing baseline Penh, a standard nebulized methacholine (MCh) challenge was performed *in situ* (0.1–100 mg/ml in saline; 3-minute Penh recorded per dose). Increases in Penh in response to MCh inhalations were first recorded in naïve animals, and 24 hours later the recordings were repeated after the treatment by inhalation of the nebulized compounds, and consequent changes in Penh were expressed as ΔPenh.

Polycation-Induced AHR. Poly-L-arginine (PLA), a mimetic of eosinophil major basic protein, activates the CaSR and induces AHR in mice after inhalation (Yarova et al., 2015). Mice were exposed to nebulized PLA (6 μM in 0.2% DMSO in PBS), PLA + CaSR NAM, or vehicle for 30 minutes immediately before MCh challenge (0.1–100 mg/ml). In separate studies to determine the drug duration of effects (PD), animals were exposed to aerosolized calcilytics or vehicle 0, 1, 2, 4, 8, or 24 hours prior to PLA treatment.

Determination of the Effects of CaSR NAMs in an Acute Asthma Model. Mice were sensitized with ovalbumin (OVA) from chicken eggs on days 0 and 5 using an intraperitoneal injection of OVA (100 μg/mouse) in 10% (50 mg/mouse) aluminum hydroxide in PBS as previously described (Yarova et al., 2015). Fourteen days after the second injection, mice were challenged by inhalation of 0.5% OVA aerosol for 1 hour twice on the same day, 4 hours apart. CaSR NAMs or corresponding vehicle treatments were administered via nebulization 1 hour prior to the first and 4 hours after the final OVA challenge. At the end of the experiments, the mice were euthanized humanely as described above, and bronchoalveolar lavage fluid (BALF) was collected as previously described (Yarova et al., 2015) and analyzed for cell numbers using a Luna FL automated cell counter (Labtech, Heathfield, United Kingdom). Lung sections were Masson trichrome-stained, and quantitative image analysis was carried out using TissueFAXS image analysis software (TissueGnostics, Vienna, Austria).

Systemic Effects of Repeated Inhaled Calcilytic Exposure. Because DMSO may accumulate in tissues with repetitive dosing, the vehicle in these experiments was changed to 0.3% propylene glycol in PBS (for NPSP-795, Ronacaleret, and JTT-305) or 0.27% propylene glycol + 0.03% ethanol in PBS (for AXT-914). Mice were placed in a Perspex chamber and exposed to nebulized CaSR NAMs or vehicle

for 1 hour daily for 5 days. After the final exposure, blood pressure and heart rate were measured as described previously using CODA noninvasive blood pressure measurement system (Kent Scientific) (Schepelmann et al., 2016). At the end of the experiment, the animals were euthanized humanely, and BALF was collected for determination of inflammatory cellular infiltration. Because the CaSR is the master controller of systemic Ca²⁺ concentrations, blood samples were also collected at the end of the experiments to measure free ionized serum Ca²⁺ concentrations as an indication of a possible systemic drug overspill after CaSR NAM nebulization.

PK. PK studies were carried out by Axis BioServices Ltd. (Coleraine, Londonderry, Northern Ireland) after direct intratracheal instillation of CaSR NAMs into anesthetized (100 mg/kg ketamine and 10 mg/kg xylazine) BALB/c mice (Penn-Century aerosolizer, Heathfield, United Kingdom). Compounds were resuspended in solution containing 3% DMSO dissolved in water containing 5% ethanol (EtOH) and 5% glucose, all at nominal concentrations of 17.5 μg/kg then filtered through a 0.45-μm pore filter, and the filtered solution was administered to the mice (Table 1). Intratracheal cassettes were dosed as a solution of 38 μg/kg (NPSP-795, Ronacaleret, and AXT-914) or 26 μg/kg (JTT-305). Whole blood (150 μl) was collected at each time point using a lateral tail vein bleed into microvettes coated with K₂EDTA. Plasma was collected by centrifugation at 2000g for 5 minutes. Animals were then humanely killed, and the lungs and trachea were removed and snap-frozen. Samples were analyzed by XenoGesis (BioCity), wherein concentrations of the tested compounds were determined using a ThermoTM TSQ Quantiva and Vanquish UHPLC system (Fisher, United Kingdom).

Head-to-Head Comparison of Inhaled CaSR NAM and ICSs in a Chronic Asthma Model. ICSs are recommended as a first line of defense for the treatment of persistent asthma in all guidelines (Ye et al., 2017; Chipps et al., 2020). The anti-inflammatory and anti-remodeling effects of the CaSR NAM NPSP-795 were compared with those of inhaled fluticasone propionate (FP) in a murine surrogate of Th2/IgE-driven asthma. Mice were initially sensitized on days 0 and 10 by intraperitoneal injection of 50 μg OVA and 50 mg aluminum hydroxide in PBS and then challenged every other day from day 21 to day 30 with inhaled 0.5% OVA delivered by aerosol for 1 hour. From day 25, mice were treated with the aerosolized NPSP-795 (6 μM), FP (0.25 mg), or vehicle (0.01% Tween-80/0.03% DMSO) delivered twice daily for 15 minutes, 1 hour prior to and 7 hours after each OVA challenge for 6 days. At the end of the experiment, the BALF was collected and analyzed as described above, whereas the lungs were infused with normal buffer formalin, formalin-fixed, paraffin-embedded, and 5-μm sections were cut for Masson's trichrome and hematoxylin and eosin staining and immunohistochemical analysis.

Crystallization and Phase Characterization

Samples of NPSP-795, Ronacaleret, and AXT-914 were crystallized after dissolution in acetone, and this was followed by slow evaporation of the solvent at room temperature over several days. AXT-914 was also crystallized from ethanol after the same procedure. For structural characterization, single crystal data were recorded on an Agilent SuperNova Dual Atlas diffractometer (Agilent, Santa Clara, CA) equipped with an Oxford Cryosystems cooling apparatus (Oxford Cryosystems, Oxford, United Kingdom). Crystal structures were solved and refined using SHELXS and SHELXL (Sheldrick, 2008, 2015). Data collection and refinement parameters are shown in Supplemental Table 1. Cambridge Crystallographic Data Centre 1915994–1915996 contain the supplementary crystallographic data for this paper. These data can be obtained free of charge from The Cambridge Crystallographic Data Centre via www.ccdc.cam.ac.uk/structures. Samples of NPSP-795 and AXT-914 crystallized from acetone and AXT-914 crystallized from ethanol were ground to a fine powder in a mortar and pestle, and their powder diffraction patterns were recorded using the same equipment.

TABLE 1

Compound characteristics, in vitro potencies, and in vivo PK parameters for all tested calcilytics

IC₅₀ and IC₈₀ values were calculated by nonlinear regression (variable slope) of conc.-response curves to CaSR NAMs obtained using measurements of intracellular Ca²⁺ as a readout for CaSR activation (by Ca²⁺) and inhibition (by CaSR NAMs) in HEK-CaSR. Plasma and lung maximal conc. (C_{max}), time of maximal conc. (T_{max}), time of 50% maximal conc. (t_{1/2}), area under the curve (AUC_{all}), and lung:plasma ratio were obtained in mice after intratracheal instillations of the tested compounds (nominal conc. of each compound: 17.5 µg/kg).

	NPSP-795	Ronacaleret	JTT-305	AXT-914
Molecular weight	436.5	447.5	514	487.4
Formula weight	473	483.9	563	487.4
Salt	HCl	HCl	0.5 H ₂ SO ₄	—
IC ₅₀ , nM	5.2	6.8	2.7	1.1
IC ₈₀ , nM	21.1	23.0	21.2	22.1
Plasma t _{1/2} , h	1.1	1.5	3.4	2.4
Plasma T _{max} , h	0.3	0.3	0.5	0.3
Plasma C _{max} , ng/ml	6.4	4.9	118.0	4.2
Plasma AUC _{all} , ng·h/ml	12.4	9.3	404.1	5.3
Lung t _{1/2} , h	1.0	1.2	0.9	0.6
Lung T _{max} , h	0.3	0.1	0.5	0.5
Lung C _{max} , ng/g	457.5	287.3	164.0	560.3
Lung AUC _{all} , ng·h/g	511.1	331.6	269.3	1250.5
Lung:plasma ratio (AUC _{all})	41.2	35.7	0.7	234.0

Estimation of Lung Deposited Dose, Allometric Scaling in Humans, Formulation, and Drug Stability Studies

These studies were performed by Cardiff Scintigraphics (Cardiff, United Kingdom) using 1 mM aqueous alcoholic solutions of CaSR NAMs in propylene glycol (PG) followed by a 300-fold dilution into PBS for NPSP-795, Ronacaleret, and JTT-305 (final drug concentrations, 3 µM; final propylene glycol content, 0.3%); AXT-914 was insoluble in propylene glycol, so it was dissolved in propylene glycol 0.27% + ethanol 0.03%. Because of the structural similarities between NPSP-795 and Ronacaleret, further analysis was carried out on only the amino alcohol NPSP-795 and the structurally unrelated quinazolin-2-one AXT-914. For the full methods, please see the Supplemental Materials.

Given the volume of the exposure chamber (15.2 l), the inhaled fraction (estimated from the fine particle fraction, of which 86.59% of particles were <3 µm in diameter), the respiratory minute volume of BALB/c mice (0.024 l/min, determined from a tidal volume of 0.15 ml and a respiratory rate of 160 breaths/min), and the duration of exposure used in the pharmacology studies (60 minutes), this equates to an atmospheric concentration of NPSP-795 of 0.69 µg/l. To correct for the 3 µM concentration used in the pharmacology studies, a value of 0.0069 µg/l is used in the equation. Using these values gives an estimated lung dosage of ~9 ng of NPSP-795 in a BALB/c mouse from nebulization of a 3 µM solution over 60 minutes.

The estimated human dosage of NPSP-795 varies from 2 µg using allometric (body surface area) scaling to 28 µg using theoretical scaled lung weight, 30 µg using scaled body weight, and 58 µg using reported lung weights. From these estimates, a value of ~30 µg was selected as a basis for the formulation stability studies.

Nebulizer solutions with a concentration of 0.4 mg/ml were prepared since only approximately 10% of the amount of drug in the nebulizer (i.e., 100 µg) is likely to be deposited in the lung in human studies. For solubility and stability testing, 2 mg of NPSP-795 were dissolved in either 100 µl of absolute EtOH or 150 µl of PG, and aliquots were kept in different storage conditions. Subsequently, 1 ml of 0.9% w/v NaCl was added to the NPSP-795 in EtOH or PG, and both formulations were subjected to 20-minute centrifugation (SciSpin One Compact Centrifuge; SciQuip Ltd.) at 2000 rpm before sampling the clear solutions. Approximately 1.5 ml of the EtOH and PG NPSP-795 in NaCl solutions was transferred into three separate Eppendorf tubes before storing at ambient room temperature 5°C and at 40°C/75% relative humidity. At each time point, 25 µl of this sample was transferred to a 10-ml volumetric flask and diluted to volume with high-performance liquid chromatography Recovery Solution (30% acetonitrile). Two-milliliter samples were transferred to high-performance liquid chromatography vials for analysis.

The solubility of 400 µg/ml AXT9-14 in EtOH and PG was comparable and required high concentrations of cosolvent to ensure complete solubility, illustrating the poor solubility of AXT-914 in both aqueous EtOH and PG solutions. To ensure complete solubility of AXT-914 in aqueous EtOH solutions requires EtOH to be at an approximate minimum concentration of 53% v/v. For toxicology studies, this value would need to be increased to at least 60% v/v to reduce the potential for precipitation during nebulization. However, as a nebulizer formulation this currently exceeds approved levels for human use. In aqueous PG solutions, an approximate minimum concentration of 71% w/w was estimated to ensure complete solubility of AXT-914. For toxicology studies, the use of a 100% PG nebulizer formulation is likely to be needed, indicating that neither EtOH nor PG solutions can be generated for human studies with AXT-914. Therefore, it may be preferred to formulate AXT-914 as a dry power inhaler formulation.

AXT-914 Micronization and Characterization of the Milled Material

Next, we tested the suitability of AXT-914 for pulmonary administration as a dry powder inhaler by testing 1) whether AXT-914 could be micronized into particles of respirable size (around 3 µm) and 2) whether the micronized material was crystalline, thermally stable, inert, and nonhygroscopic. For the full methods, please see the Supplemental Materials.

Quantification of Airway Remodeling

Quantitative image analysis was performed using StrataQuest image analysis software (TissueGnostics) (). An average of 16 smaller airways (<40,000 µm²; n = 3–21) were examined from three to four Masson's trichrome-stained lung sections from each animal (n = 6 per condition) for assessment of remodeling markers within manually identified regions of interest (Supplemental Fig. 7, A and B). Manual airway object identification was performed by operators blinded to the experimental conditions using the Opensource blindrename.pl script (Slater, 2016).

Statistical Analysis

Statistical analysis was undertaken with GraphPad Prism 7 software (GraphPad Software), and sample size and all analysis steps were decided before the data had been gathered. Data are expressed as mean and S.D. Student's two-tailed unpaired or paired *t* tests were used to compare two data sets; one- or two-way ANOVA with an

appropriate *post hoc* test as stated in the figure legends was used for multiple comparisons.

Results

Determination of CaSR NAM Efficacies and Potencies. All calcilytics examined concentration-dependently suppressed CaSR-mediated increases in intracellular Ca^{2+} induced by 5 mM extracellular Ca^{2+} in HEK-CaSR cells (Fig. 1). The CaSR NAMs previously tested in the clinic, NPSP-795, Ronacaleret, AXT-914, and JTT-305, with estimated 80% inhibitory concentration (IC_{80}) values of around 20 nM, were all 10 times more potent than the laboratory-grade NAM, NPS2143 ($\text{IC}_{80} = 202$ nM; Table 1). Based on lung dosage estimates (see relevant *Methods* section) and total mouse lung capacity of 1 ml, this may be roughly approximated to stock solutions of 3 μM for the clinically tested calcilytics and 25 μM for the positive control NPS2143 for *in vivo* experiments.

CaSR NAMs Induce Airway Relaxation in Isolated Naïve Mouse Airways. The next steps were to investigate the effects of CaSR NAMs on airway contractility by measuring tension changes of naïve mouse tracheae half-maximally contracted with ACh in medium containing 2 mM Ca^{2+} to mimic proinflammatory conditions. Figure 2 shows that the DMSO vehicle applied at the tracheae precontracted with ACh at concentrations matching those used to dissolve the CaSR NAMs evoked a concentration-dependent increase in the tracheal tone (up to $+23.6\% \pm 7.8\%$ from the steady-state ACh-induced tone). In contrast, all CaSR NAMs tested relaxed precontracted mouse tracheae at concentrations of 100 nM or greater [up to -30.7% (NPSP-795, $N = 5$), -25.2% (JTT-305, $N = 3$), -46.8% (Ronacaleret, $N = 5$), -30.8% (AXT-914, $N = 4$) at 30 μM] from the corresponding level of tone induced by the DMSO vehicle). CaSR NAMs were still able to relax precontracted tracheae in the presence of medium containing physiologic Ca^{2+} concentrations (i.e., 1 mM), albeit less effectively than in proinflammatory conditions (Supplemental Fig. 1). No CaSR NAM evoked constriction in the presence of medium containing either physiologic (Supplemental Fig. 2) or pathologic (Fig. 2) Ca^{2+} levels.

Topical Delivery of Structurally Unrelated Inhaled CaSR NAMs Suppresses AHR and Inflammation in Mice. As previously demonstrated (Yarova et al., 2015), exposure of naïve mice to the polycation PLA increased MCh responsiveness (Fig. 3A) compared with vehicle-treated animals. All nebulized CaSR NAMs (3 μM in the nebulization solution) abolished this effect of PLA (Fig. 3B). This effect was concentration-dependent (Supplemental Fig. 2). In addition, in line with our previous studies using laboratory-grade compounds (Yarova et al., 2015), prophylactic inhalation of all the tested CaSR NAMs also suppressed AHR and BALF inflammatory cellular infiltration in OVA-sensitized and challenged mice when administered prior to and after OVA challenge in the murine surrogate (Fig. 3, C and D).

Effects of CaSR NAMs on the L-Type Ca Channel. Previous studies have confirmed that CaSR NAMs are deemed safe in the clinic when delivered systemically. Since some CaSR NAMs are structural derivatives of dihydropyridines (L-type Ca^{2+} (L_{Ca}) channel blockers), we explored whether the CaSR NAMs employed in our studies untowardly affect inward, whole-cell macroscopic currents conducted through voltage-gated L_{Ca} channels, which could account for the observed CaSR NAM-mediated airway relaxation. Supplemental Fig. 3 shows that the CaSR NAMs NPSP-795, Ronacaleret, and AXT-914 (all 10 μM) had no effect on normalized L_{Ca} current compared with that measured in the presence of DMSO vehicle, whereas, as expected, nifedipine (10 μM), a classic inhibitor of L_{Ca} channels, completely abolished normalized L_{Ca} current ($P < 0.0001$; $N = 17$).

Determination of the Systemic Effects of Repeated Exposure to Inhaled CaSR NAMs. Next, we investigated the effects of repeated exposure of naïve BALB/c mice (5 days, 1 h/day) to nebulized solutions of the inhaled CaSR NAMs previously tested in clinical trials and their effects on blood pressure, heart rate, serum Ca^{2+} concentration (a surrogate for changes in plasma parathyroid hormone), and airway irritation, as reflected by BALF inflammatory cellular infiltration. Repeated administration (5 days, 1 h/day) of AXT-914 and JTT-305 but not NPSP-795 or Ronacaleret evoked an increase in the mean BALF total cell count when compared with their respective vehicle controls (from $22.7 \times 10^6 \pm 4.4 \times$

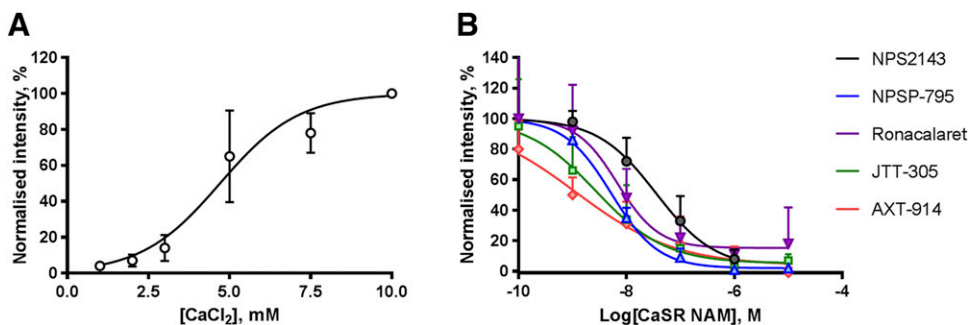


Fig. 1. Structurally unrelated amino alcohol (NPSP-795, Ronacaleret, JTT-305, and NPS2143) and quinazolin-2-one (AXT-914) CaSR NAMs inhibit the human CaSR *in vitro*. (A) Activation of the CaSR in response to increasing Ca^{2+} concentrations (0.5–10 mM) in HEK293 cells stably transfected with the human CaSR. The estimated EC_{50} value is 5 mM. (B) Inhibitory effects of cumulative additions of CaSR NAMs previously tested in the clinic (NPSP-795, Ronacaleret, JTT-305, and AXT-914) and of the positive control, NPS2143, on CaSR activation evoked by 5 mM Ca^{2+} . All CaSR NAMs previously tested in the clinic appear to be more potent than the positive control, with estimated IC_{80} values for NPSP-795, Ronacaleret, JTT-305, and AXT-914 of 20 nM, whereas for NPS2143 IC_{80} the value is 202 nM. Data are presented as mean \pm S.D.; $N = 3-9$, $n = 125-520$, wherein N is the number of independent experiments, and n is the number of individual cells.

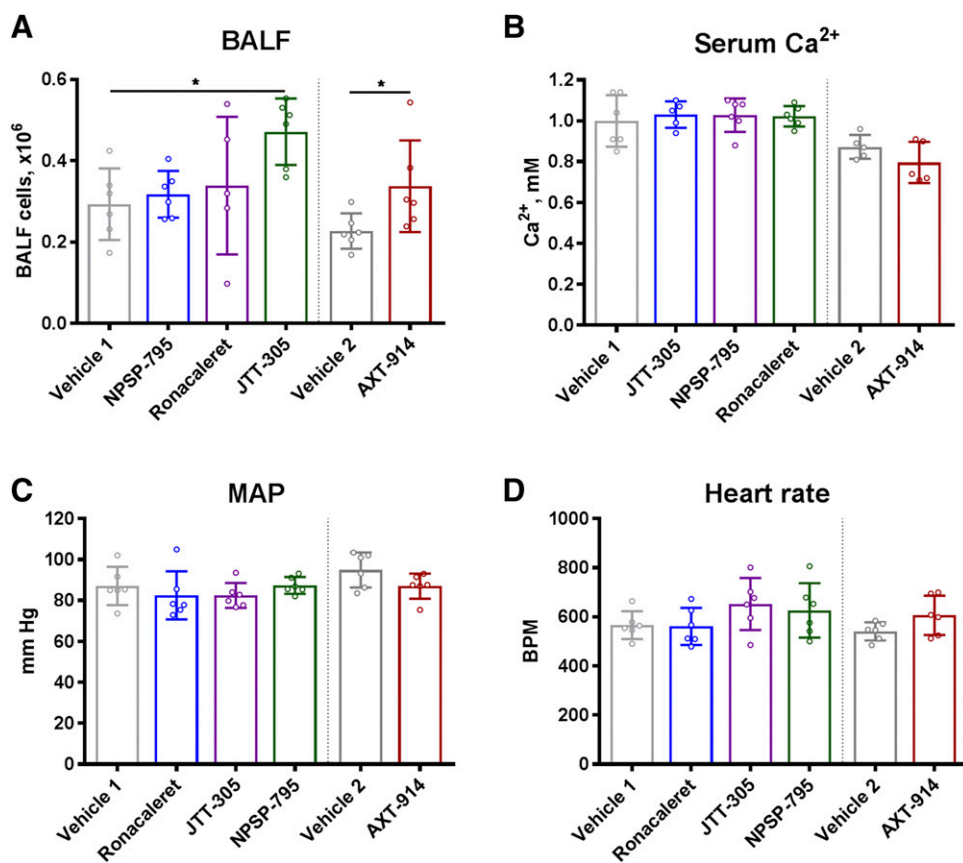


Fig. 4. Systemic effects of repeated exposure to CaSR NAM inhalations in naïve mice in vivo. Effects of repeated (5 days) exposure to inhaled CaSR NAMs previously tested in the clinic as oral drugs on (A) BALF cellular infiltration; (B) serum Ca²⁺ concentration; (C) mean arterial blood pressure (MAP); (D) heart rate [beats per minute (BPM)]. Vehicle 1: 0.3% propylene glycol in PBS. Vehicle 2: 0.27% propylene glycol + 0.03% ethanol in PBS. Data are shown as scatter dot plot \pm S.D.; $N = 5$ to 6 animals per experimental group. Statistical comparisons: ANOVA with Holm-Sidak's post hoc test (amino alcohol CaSR NAMs, NPSP-795, Ronacaleret, and JTT-305) or two-tailed unpaired T-test (quinazolin-2-one CaSR NAM, AXT-914). * $P < 0.05$; ** $P < 0.01$.

PLA inhalation (6 μ M for 30 minutes), which was immediately followed by MCh challenge. NPSP-795 abrogated diminished PLA-induced AHR for up to 8 hours after treatment (Fig. 6A) but was ineffective by 24 hours. AXT-914 abrogated PLA-induced AHR 2 hours but not 8 hours or more after nebulized delivery (Fig. 6B).

Crystallography of CaSR NAMs. The amino alcohol NPSP-795 crystallized from acetone as the hydrochloride (Supplemental Fig. 4; Supplemental Table 1). Powder diffraction showed that the crystal structure was consistent with the bulk of the recrystallized sample. A later crop of crystallization material revealed the presence of an additional but unidentified phase, which could be a new polymorph or a solvate. Grinding a sample of the pure material resulted in some loss in crystallinity but no phase transformation (Supplemental Fig. 4).

The amino alcohol Ronacaleret crystallized from acetone because the hydrochloride and the crystal structure obtained was the same as that previously reported (Supplemental Table 1) (Vogt et al., 2014).

The crystals of AXT-914 obtained from acetone revealed the existence of a new single phase before and after grinding (Supplemental Fig. 5, A and B; Supplemental Table 1) consisting of four independent molecules with a range of conformations. Comparison of the powder X-ray diffraction data recorded for the sample with the pattern simulated from the single crystal data showed that the sample was a single phase. The powder pattern recorded for the sample before recrystallization indicated the existence of a different but yet to be identified phase, possibly a polymorph or solvate. Grinding

the recrystallized sample did not reveal a change in phase (Supplemental Fig. 5B). Crystals of AXT-914 existed in two distinct phases according to whether they had been crystallized from ethanol or acetone. Both were resistant to grinding (Supplemental Fig. 5C).

Formulation Studies for the Amino Alcohol NPSP-795 and the Quinazolin-2-one AXT-914 CaSR NAMs. For NPSP-795, the data provide confidence that a simple nebulizer solution can be prepared for use by a clinical research organization, and the stability of such solutions will permit daily dosing in a standard schedule. Follow-up studies have shown physical stability in 5% solutions of either EtOH or PG with chemical stability for at least 6 hours when refrigerated, which is compatible with human use.

In contrast, AXT-914 demonstrates poor solubility in both aqueous EtOH or PG solutions and for routine use in humans would likely require formulation either as a nebulizer suspension or as a dry power inhaler formulation. In both circumstances, the AXT-914 powder would need to be micronized to around 2 to 3 μ m before formulation studies could proceed. Therefore, the next steps were to investigate the possibility that AXT-914 could be micronized into particles of respirable size.

AXT914 Micronization, Particle Size Determination, and Stability. The particle size was assessed to ensure adequate size for lung deposition, with an average particle size of 1 to 6 μ m. After jet milling AXT-914 and using laser diffraction, a monodispersed distribution could be observed (Supplemental Fig. 6A, left), with half maximum distribution D(50) of 3.59 μ m (Supplemental Fig. 6A, right). The size of

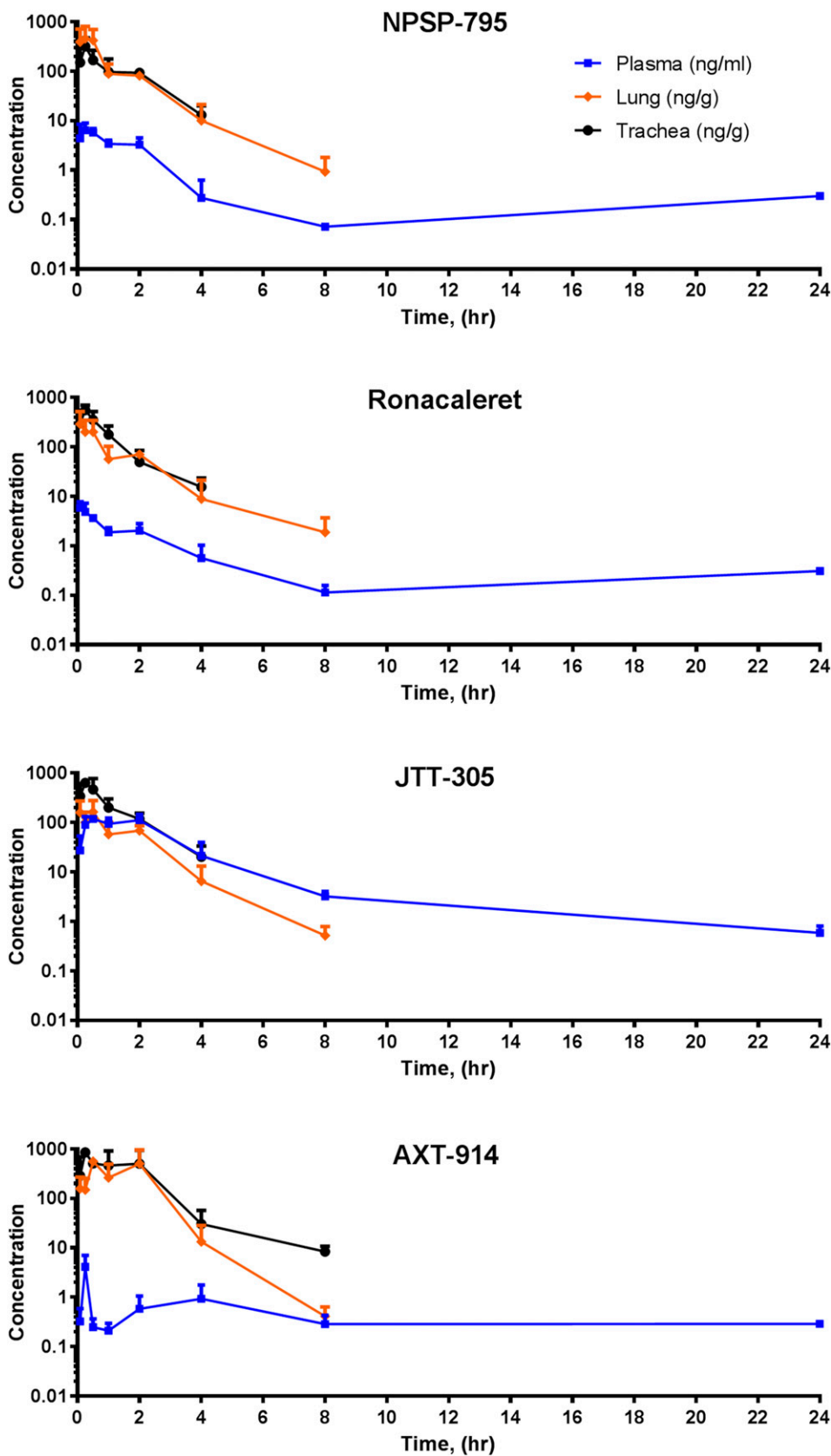
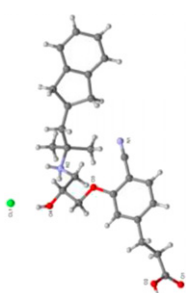
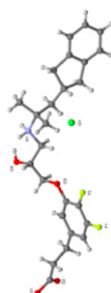
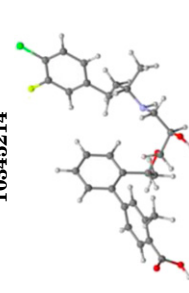


Fig. 5. Pharmacokinetics of CaSR NAMs in naive mice in vivo. Retention times in murine blood plasma (blue), lung (orange), and trachea (black) after intratracheal instillations of CaSR NAMs previously tested in the clinic. Compounds were resuspended in 3% DMSO, 97% (5% EtOH/5% glucose in water) at a concentration of 17.5 $\mu\text{g}/\text{kg}$ and then filtered through a 0.45- μm pore filter, and the filtered solution was administered to the mice. Data are shown as the mean \pm S.D.; $N = 1\text{--}3$ animals per each time point.

TABLE 2

CaSR NAMs previously developed for systemic use and tested in humans potentially available for repurposing as inhaled asthma drugs
 Development compound table illustrating compound code, development company, chemical structure, molecular weight (MW), crystal structures, developmental stages and number of patients, duration, and references to the clinical trials. NPSP-795, Ronacaleret, JTT-305, and AXT-914 crystal structures were generated as part of the current studies.

Code	Company	MW (g/mol)	Crystal Structure; PubChem CID	Development Stage	StdInChIKey; NCT; References
NPSP795/SB-423562 (amino-alcohol) NPSP790/SB-423557 (ester prodrug) NPSP795/SHP635 (amino-alcohol)	NPS/GlaxoSmithKline (osteoporosis); NPS (autosomal dominant hypocalcemia type 1)	436.5	 9910902	Phase I (<i>n</i> = 28; i.v.; two study sessions 7 days apart) (<i>n</i> = 50; oral; > two study sessions 7 days apart); phase II (<i>n</i> = 7; 17 days; i.v.)	NJBFFJCJKWWIKRD-HSZRJJFAPSA-N; https://pubmed.ncbi.nlm.nih.gov/19786130 NCT02204579; https://pubmed.ncbi.nlm.nih.gov/31063613
Ronacaleret/SB-751689 (amino-alcohol)	GlaxoSmithKline (osteoporosis)	447.5	 10345214	Phase II (<i>n</i> = 569; 12 mo; oral)	FQJISUPNNMFRIFZ-HXUWFFJFHSA-N; NCT00471237; https://pubmed.ncbi.nlm.nih.gov/23756230
JTT-305/MK-5442; Encalaret (amino alcohol)	Japan Tobacco/Merck (osteoporosis)	514	 46917559	Phase II (<i>n</i> = 526; 12 mo; oral)	UNFHDRVFEQPUEL-DENIHFKOSA-N; NCT00996801; https://pubmed.ncbi.nlm.nih.gov/26556736
AXT914 (quinazolin-2-one)	Novartis (osteoporosis)	487.4	Not applicable.	Phase II (<i>n</i> = 105; 4 wk; oral)	NCT00417261; https://pubmed.ncbi.nlm.nih.gov/24769332

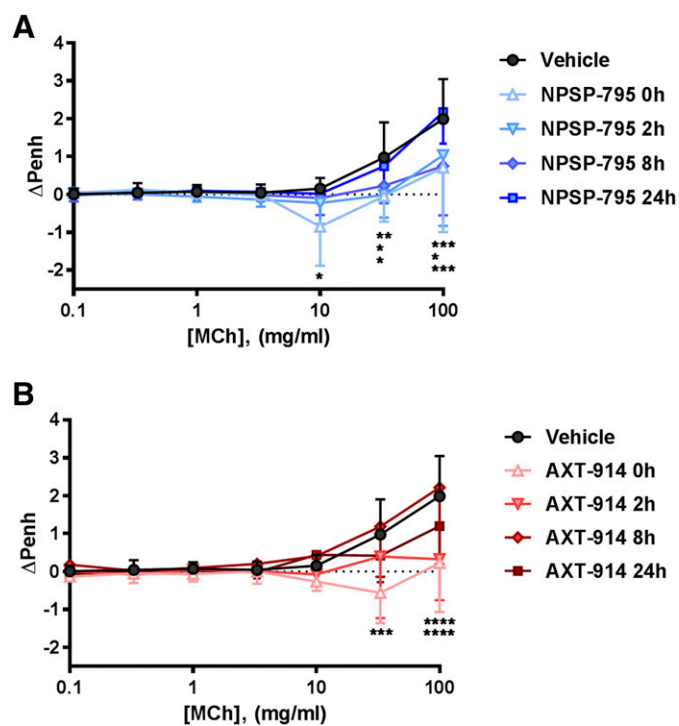


Fig. 6. Pharmacodynamics of amino alcohol (NPSP-795) and quinazolin-2-one (AXT-914) CaSR NAMs in naive mice in vivo. Effects of NPSP-795 (A) or AXT-914 (B) pretreatment (0, 2, 8, or 24 hours) on PLA-induced increase in Δ Penh. Vehicle: 0.1% DMSO in PBS. Data are shown as mean \pm S.D.; $N = 5$ –9 animals per experimental group. Statistical comparisons: ANOVA with Dunnett's post hoc test. * $P < 0.05$; ** $P < 0.01$; *** $P < 0.001$; **** $P < 0.0001$.

both raw and micronized particles was confirmed using scanning electron microscopy, as shown in Supplemental Fig. 6B. Using the scanning electron microscopy scale tool, 27 random particles were measured and ranged from 1.04 to 4.38 μm , with average size of $2.22 \pm 0.75 \mu\text{m}$. The thermal response of the milled material showed an endothermic peak at 125°C indicative of the melting temperature of AXT-914, whereas the exothermic peak at 270°C may be related to the thermal degradation of the substance (Supplemental Fig. 6C). Representative moisture sorption isotherms as a function of relative humidity (%) are shown in Supplemental Fig. 6D. A minimal weight gain of 0.2% was observed between 0% and 90% relative humidity, indicating that milled AXT-914 is crystalline.

Head-to-Head Comparison of the Anti-Inflammatory Activities of Inhaled CaSR NAM and Inhaled Corticosteroid in a Chronic Murine Asthma Surrogate. Because the CaSR NAM NPSP-795 is suitable for nebulization, whereas AXT-914 requires the development of a dry powder inhaler before further testing in rodent models and in humans can be undertaken, NPSP-795 alone was used in the head-to-head comparison against the current standard-of-care experiments. We developed a murine asthma surrogate based on OVA sensitization and challenge (Fig. 7A) in which we tested the effects of repeated exposure to inhaled NPSP-795 against those of the standard of care, FP. Concomitant, repeated exposure to nebulized NPSP-795 or FP during the later phases of serial OVA inhalation challenge in the OVA-sensitized mice, which was associated with a significant elevation of the mean numbers of total cells and eosinophils in the BALF,

significantly reduced the mean total cell and eosinophil counts to a comparable degree (Fig. 7B). Quantitative image analysis revealed that NPSP-795 inhalation reduced the mean goblet cell number in the airways, whereas FP did not (Fig. 7C). Other remodeling parameters, such as total tissue, epithelial tissue, and airway size, were all unaffected (Supplemental Fig. 7, C and D).

Discussion

In our previous study (Yarova et al., 2015), we presented data compatible with the hypothesis that bronchial smooth muscle hyperresponsiveness, which is the quintessential feature of human asthma, is caused at least in part by elevated expression and/or activation of the CaSR on airway smooth muscle cells, resulting in a heightened response to a contractile stimulus, and that blockade of the CaSR with CaSR NAMs, also known as calcilytics, abolishes it. Here we address the practicability of repurposing a range of NAMs previously tested in clinical trials of osteoporosis therapy and administered systemically for their suitability for topical application for asthma therapy using dosing regimens and inhaler-delivered, topical formulations resembling those in current clinical use. To this end, we employed animal surrogates in which the CaSR on airway smooth muscle cells was stimulated artificially with nebulized PLA, a CaSR activator, or in which animals were sensitized and challenged with OVA to create asthma-like airway inflammation.

In many asthmatics, bronchial smooth muscle hyperresponsiveness is further complicated by the coexistence of airway inflammation. Our earlier studies also revealed that products of inflammatory cells typically involved in airway inflammation in asthma, such as eosinophils and neutrophils, may directly exacerbate bronchospasm in patients with bronchial smooth muscle hyperresponsiveness by releasing polycations (e.g., eosinophil cationic proteins, major basic proteins, or polyamines), which are direct agonists at the CaSR (Yarova et al., 2015). This is a previously known but mechanistically unexplained positive feedback mechanism for asthma exacerbation by the products of inflammatory cells, which we have shown is abolished by topical CaSR NAM therapy (Yarova et al., 2015; Corrigan, 2020). In addition, inflammation, by causing swelling of the airway lining with edema, greatly amplifies the obstruction caused by a given degree of smooth muscle contraction. Topical and systemic corticosteroids ameliorate asthma not by targeting bronchial smooth muscle hyperresponsiveness but by reducing infiltration of the airway with inflammatory cells that produce CaSR agonists and by reducing edema and swelling of the airway mucosa, thus increasing their internal diameter (Chan and Silverman, 1993; Baraldi et al., 2005; Carraro et al., 2010). Corticosteroids may also enhance the effects of bronchodilators (Koziol-White et al., 2020). Studies suggesting that corticosteroids reduce hyperresponsiveness of the asthmatic airway over time (Lundgren et al., 1988; Jeffery et al., 1992; Laitinen and Laitinen, 1995) most likely reflect the fact that they reduce airway mucosal inflammation and edema progressively and prophylactically in those asthmatics who evince a significant amount of this inflammation, although they are ineffective against the underlying phenomenon of bronchial smooth muscle hyperresponsiveness. These data suggest that inhaled CaSR NAMs represent the first antiasthma therapy

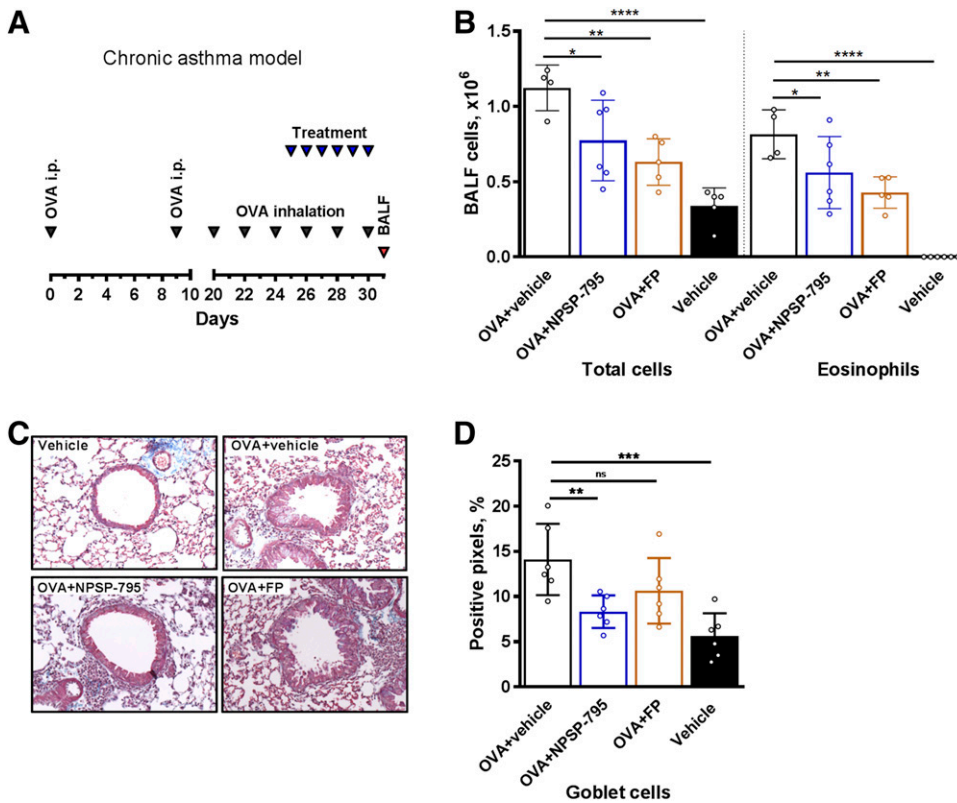


Fig. 7. Head-to-head comparison of inhaled CaSR NAMs or FP treatment on BALF inflammation and remodeling in a therapeutic asthma model. (A) Schematic exposure protocol. (B) Balb/c mice were sensitized and challenged with OVA, and the effects of inhaled NPSP-795 or inhaled FP were determined on BALF total leukocyte (left panel) and eosinophil cell count (right panel) at the end of the experiment. $N = 4-6$ animals per experimental group. (C) Representative images of Masson's trichrome-stained lung sections. (D) The effects of inhaled NPSP-795 or FP on goblet cells were quantified using StrataQuest image analysis software as described in Supplemental Fig. 7. Data are shown as scatter dot plot \pm S.D., with $N = 6$ animals per experimental group, and $n = 3-21$ airways from three to four Masson's trichrome-stained lung sections per animal. Statistical comparisons: one-way ANOVA with Holm-Sidak's post hoc test. * $P < 0.05$; ** $P < 0.01$; *** $P < 0.001$; **** $P < 0.0001$. ns, not significant.

with the potential not only to abolish bronchial smooth muscle hyperresponsiveness [and not simply temporarily antagonize its effects, as seen with bronchodilators (Bourke et al., 2019)] but also to reverse bronchial mucosal inflammation and edema and the local overproduction of CaSR agonists by inflammatory cells. Thus, they offer the possibility of much more comprehensive asthma control with a single, nontoxic, nonsteroidal topical drug.

The CaSR is widely expressed on structural and inflammatory cells of the airway. CaSR NAMs function as upstream inhibitors of many signaling processes, including those that result in the release of inflammatory mediators (Lee et al., 2012, 2017a,b; Yarova et al., 2015). In the present study, we show that a range of CaSR NAMs previously tested in clinical settings administered directly to the airway abolish PLA-induced AHR, inhibit the airway inflammatory response associated with OVA sensitization, and challenge at least as well as topical corticosteroids. This highlights a class-specific effect of these drugs and firmly supports the hypothesis that the observed anti-inflammatory properties reflect blockade of the CaSR. In addition, NPSP-795 reduces goblet cell hyperplasia in a chronic asthma model. These results concur with previously published observations that CaSR NAMs suppress mucus secretion in tobacco smoke-stimulated human epithelial cells (Lee et al., 2017b), suggesting that chronic use of inhaled CaSR NAMs might preserve airway structure over time and prevent irreversible airway blockage through remodeling. Notably, CaSR NAMs evoke small relaxation of isolated murine airways independently of their class, and this relaxation is not due to the off-target inhibition of L-type Ca^{2+} channels.

Systemic CaSR NAMs were developed to evoke pulsatile changes in plasma parathyroid hormone, an established bone

anabolic stimulus. Despite good safety and tolerability profiles in osteoporosis clinical trials (Widler, 2011; Halse et al., 2014), some patients developed hypercalcemia. To obviate this issue, topical, inhaled CaSR NAM therapy for asthma should ideally result in topically effective airway concentrations with minimal systemic absorption (Lötval, 1997). Our data, albeit in laboratory animals, suggest that topical application of the clinical-grade CaSR NAMs in concentrations likely to be therapeutically relevant for asthma therapy does not derange calcium metabolism or exert any detectable cardiorespiratory unwanted effects. Repeat exposure of naïve mice to either NPSP-795 or Ronacaleret did not cause airway irritancy, whereas JTT-305 and AXT-914 slightly increased the mean number of cells in the BALF of naïve animals, suggesting a possible effect on cellular migration or capillary permeability after drug nebulization of these two compounds when applied topically to the airway. However, this potential issue might putatively be overcome by delivery using conventional, antiasthma metered-dose inhalers or dry powder, microparticle suspensions as distinct from nebulized solutions.

In PK studies in mice, NPSP-795, Ronacaleret, and AXT-914 were cleared from the lungs within 8 hours with minimal systemic exposure after intratracheal dosing, indicating that in humans these molecules might be suitable for twice-daily, topical application. In contrast, JTT-305 showed substantial retention in the circulation, detracting from its suitability for topical repurposing. In addition, our data confirm lack of off-target effects of NPSP-795, Ronacaleret, and AXT-914 at the dihydropyridine-sensitive L-type Ca^{2+} channels expressed in the cardiovascular system (Bodi et al., 2005).

Since NPSP-795 and Ronacaleret are structurally very similar, further studies were carried out using the amino

alcohol NPSP-795 and the quinazolin-2-one AXT-914. Pharmacodynamically, NPSP-795 abrogated PLA-induced bronchial smooth muscle hyperresponsiveness for at least 8 hours after topical application but was ineffective (presumably reflecting elimination) within 24 hours. AXT-914, in contrast, exhibited a shorter duration of action, although PK studies demonstrated that it was retained longer in the trachea. Formulation studies provide confidence that for NPSP-795, a simple nebulizer solution can be prepared for first-in-human studies in conditions typically found in a clinical research organization, and the stability of such solutions will permit daily dosing in a standard schedule. The estimated human dosage for NPSP-795 is 30 μg , which is comparable to many other inhaled asthma drugs.

In contrast, AXT-914 is insoluble in solvents commonly used in clinical settings, requiring further formulation development. Crystallization and micronization studies show that AXT-914 retains a single phase in different crystallization solvents, and it can be milled into particles of respirable size ranging between 2 and 3 μm ; thus it is potentially suitable for inhaled delivery. The structure of the jet-milled AXT-914 is crystalline and chemically stable, indicating suitability of the micronized material as a nebulized suspension or a dry powder formulation.

In summary, these preclinical data support the hypothesis that NPSP-795, and AXT-914, after formulation refinement, have suitable pharmacological, PK/PD, and safety profiles appropriate for topical administration to human patients with asthma. Current management of refractory asthma requires therapy with bronchodilators and topical and systemic anti-inflammatory corticosteroids and, recently, “biological” therapies, all of which raise concerns or questions of safety, efficacy, unwanted effects, compliance, logistics, and cost. Successful delivery of CaSR NAMs to the airway promises to eliminate bronchial smooth muscle hyperresponsiveness and thus spontaneous constriction of the asthmatic airway, rendering routine use of bronchodilators redundant and inhibiting airway inflammation in a corticosteroid-independent fashion. In addition, long-term use of topical CaSR NAM therapy may prove to alter the natural history of irreversible airway obstruction.

In conclusion, inhaled CaSR NAMs could provide a first-in-class, single topical therapy for asthma in children and adults, simultaneously eliminating airway smooth muscle hyperresponsiveness and reducing airway inflammation and remodeling safely, efficiently, and in a cost-effective manner.

Acknowledgments

The authors wish to thank Glyn Taylor (Cardiff University and Cardiff Scintigraphics) and Richard Weaver (Xenogenesis) for helpful discussions as well as the late Chris Peers for the gift of the HEK293 cells stably transfected with the $\alpha 1\text{c}$ subunit of L-type Ca^{2+} channels.

Authorship Contributions

Participated in research design: Yarova, Huang, Ecker, Nica, Telezhkin, Kidd, Ford, Broadley, Kemp, Riccardi.

Conducted experiments: Yarova, Huang, Schepelmann, Bruce, Telezhkin, Gomes dos Reis, Riccardi.

Contributed new reagents or analytic tools: Traini, Kariuki.

Performed data analysis: Yarova, Bruce, Telezhkin, Traini, Kariuki, Riccardi.

Wrote or contributed to the writing of the manuscript: Yarova, Kidd, Ford, Corrigan, Ward, Riccardi.

References

- An SS, Bai TR, Bates JH, Black JL, Brown RH, Brusasco V, Chitano P, Deng L, Dowell M, Eidelman DH, et al. (2007) Airway smooth muscle dynamics: a common pathway of airway obstruction in asthma. *Eur Respir J* **29**:834–860.
- Baraldi E, Bonetto G, Zucchello F, and Filippone M (2005) Low exhaled nitric oxide in school-age children with bronchopulmonary dysplasia and airflow limitation. *Am J Respir Crit Care Med* **171**:68–72.
- Blacquièrre MJ, Hylkema MN, Postma DS, Geerlings M, Timens W, and Melgert BN (2010) Airway inflammation and remodeling in two mouse models of asthma: comparison of males and females. *Int Arch Allergy Immunol* **153**:173–181.
- Bodi I, Mikala G, Koch SE, Akhter SA, and Schwartz A (2005) The L-type calcium channel in the heart: the beat goes on. *J Clin Invest* **115**:3306–3317.
- Bourke C, Everard M, Devadason S, Ditcham W, and Depiazzi J (2019) Controlled inhalation improves total and peripheral lung deposition in CF. *Eur Respir J* **54**: PA4527.
- Brennan SC, Wilkinson WJ, Tseng HE, Finney B, Monk B, Dibble H, Quilliam S, Warburton D, Galiotta LJ, Kemp PJ, et al. (2016) The extracellular calcium-sensing receptor regulates human fetal lung development via CFTR. *Sci Rep* **6**: 21975.
- Brown EM, Gamba G, Riccardi D, Lombardi M, Butters R, Kifor O, Sun A, Hediger MA, Lytton J, and Hebert SC (1993) Cloning and characterization of an extracellular Ca^{2+} -sensing receptor from bovine parathyroid. *Nature* **366**:575–580.
- Caltabiano S, Dollery CT, Hossain M, Kurtinez MT, Desjardins JP, Favus MJ, Kumar R, and Fitzpatrick LA (2013) Characterization of the effect of chronic administration of a calcium-sensing receptor antagonist, ronacaleret, on renal calcium excretion and serum calcium in postmenopausal women. *Bone* **56**:154–162.
- Carraro S, Piacentini G, Lusiani M, Uyan ZS, Filippone M, Schiavon M, Boner AL, and Baraldi E (2010) Exhaled air temperature in children with bronchopulmonary dysplasia. *Pediatr Pulmonol* **45**:1240–1245.
- Chan KN and Silverman M (1993) Increased airway responsiveness in children of low birth weight at school age: effect of topical corticosteroids. *Arch Dis Child* **69**: 120–124.
- Chippis B, Taylor B, Bayer V, Shaikh A, Mosnaim G, Trevor J, Rogers S, Del Aguila M, Paek D, and Wechsler ME (2020) Relative efficacy and safety of inhaled corticosteroids in patients with asthma: systematic review and network meta-analysis. *Ann Allergy Asthma Immunol* **125**:163–170.e3.
- Corrigan CJ (2020) Calcilytics: a non-steroidal replacement for inhaled steroid and SABA/LABA therapy of human asthma? *Expert Rev Respir Med* **14**:807–816.
- Donovan C, Royce SG, Esposito J, Tran J, Ibrahim ZA, Tang ML, Bailey S, and Bourke JE (2013) Differential effects of allergen challenge on large and small airway reactivity in mice. *PLoS One* **8**:e74101.
- Fearon IM, Ball SG, and Peers C (2000) Clotrimazole inhibits the recombinant human cardiac L-type Ca^{2+} channel $\alpha 1\text{C}$ subunit. *Br J Pharmacol* **129**:547–554.
- Fernandez-Rodriguez S, Broadley KJ, Ford WR, and Kidd EJ (2010) Increased muscarinic receptor activity of airway smooth muscle isolated from a mouse model of allergic asthma. *Pulm Pharmacol Ther* **23**:300–307.
- Halse J, Greenspan S, Cosman F, Ellis G, Santora A, Leung A, Heyden N, Samanta S, Doleckyj S, Rosenberg E, et al. (2014) A phase 2, randomized, placebo-controlled, dose-ranging study of the calcium-sensing receptor antagonist MK-5442 in the treatment of postmenopausal women with osteoporosis. *J Clin Endocrinol Metab* **99**:E2207–E2215.
- Hamelmann E, Schwarze J, Takeda K, Oshiba A, Larsen GL, Irvin CG, and Gelfand EW (1997) Noninvasive measurement of airway responsiveness in allergic mice using barometric plethysmography. *Am J Respir Crit Care Med* **156**:766–775.
- Hannan FM, Kallay E, Chang W, Brandi ML, and Thakker RV (2018) The calcium-sensing receptor in physiology and in calcitropic and noncalcitropic diseases. *Nat Rev Endocrinol* **15**:33–51.
- Hansbro PM, Kim RY, Starkey MR, Donovan C, Dua K, Mayall JR, Liu G, Hansbro NG, Simpson JL, Wood LG, et al. (2017) Mechanisms and treatments for severe, steroid-resistant allergic airway disease and asthma. *Immunol Rev* **278**:41–62.
- Jeffery PK, Godfrey RW, Adelroth E, Nelson F, Rogers A, and Johansson SA (1992) Effects of treatment on airway inflammation and thickening of basement membrane reticular collagen in asthma. A quantitative light and electron microscopic study. *Am Rev Respir Dis* **145**:890–899.
- John MR, Harfst E, Loeffler J, Belleli R, Mason J, Bruin GJ, Seuwen K, Klickstein LB, Mindeholm L, Widler L, et al. (2014) AXT914 a novel, orally-active parathyroid hormone-releasing drug in two early studies of healthy volunteers and postmenopausal women. *Bone* **64**:204–210.
- Koziol-White C, Johnstone TB, Corpuz ML, Cao G, Orfanos S, Parikh V, Deeney B, Tliba O, Ostrom RS, Dainty I, et al. (2020) Budesonide enhances agonist-induced bronchodilation in human small airways by increasing cAMP production in airway smooth muscle. *Am J Physiol Lung Cell Mol Physiol* **318**:L345–L355.
- Kumar S, Matheny CJ, Hoffman SJ, Marquis RW, Schultz M, Liang X, Vasko JA, Stroup GB, Vaden VR, Haley H, et al. (2010) An orally active calcium-sensing receptor antagonist that transiently increases plasma concentrations of PTH and stimulates bone formation. *Bone* **46**:534–542.
- Kurosawa M, Shimizu Y, Tsukagoshi H, and Ueki M (1992) Elevated levels of peripheral-blood, naturally occurring aliphatic polyamines in bronchial asthmatic patients with active symptoms. *Allergy* **47**:638–643.
- Laitinen LA and Laitinen A (1995) Inhaled corticosteroid treatment for asthma. *Allergy Proc* **16**:63–66.
- Lee GS, Subramanian N, Kim AI, Aksentjevich I, Goldbach-Mansky R, Sacks DB, Germain RN, Kastner DL, and Chae JJ (2012) The calcium-sensing receptor regulates the NLRP3 inflammasome through Ca^{2+} and cAMP. *Nature* **492**: 123–127.
- Lee JW, Park HA, Kwon OK, Park JW, Lee G, Lee HJ, Lee SJ, Oh SR, and Ahn KS (2017a) NPS 2143, a selective calcium-sensing receptor antagonist inhibits lipopolysaccharide-induced pulmonary inflammation. *Mol Immunol* **90**:150–157.
- Lee JW, Park JW, Kwon OK, Lee HJ, Jeong HG, Kim JH, Oh SR, and Ahn KS (2017b) NPS2143 inhibits MUC5AC and proinflammatory mediators in cigarette

- smoke extract (CSE)-Stimulated human airway epithelial cells. *Inflammation* **40**: 184–194.
- Lötvall J (1997) Local versus systemic effects of inhaled drugs. *Respir Med* **91** (Suppl A):29–31.
- Lundgren R, Söderberg M, Hörstedt P, and Stenling R (1988) Morphological studies of bronchial mucosal biopsies from asthmatics before and after ten years of treatment with inhaled steroids. *Eur Respir J* **1**:883–889.
- Maarsingh H, Zaagsma J, and Meurs H (2008) Arginine homeostasis in allergic asthma. *Eur J Pharmacol* **585**:375–384.
- Melgert BN, Postma DS, Kuipers I, Geerlings M, Luinge MA, van der Strate BW, Kerstjens HA, Timens W, and Hylkema MN (2005) Female mice are more susceptible to the development of allergic airway inflammation than male mice. *Clin Exp Allergy* **35**:1496–1503.
- Nemeth EF, Van Wagenen BC, and Balandrin MF (2018) Discovery and development of calcimimetic and calcilytic compounds. *Prog Med Chem* **57**:1–86.
- O'Byrne P, Fabbri LM, Pavord ID, Papi A, Petruzzelli S, and Lange P (2019) Asthma progression and mortality: the role of inhaled corticosteroids. *Eur Respir J* **54**: 1900491.
- Riccardi D and Kemp PJ (2012) The calcium-sensing receptor beyond extracellular calcium homeostasis: conception, development, adult physiology, and disease. *Annu Rev Physiol* **74**:271–297.
- Rossol M, Pierer M, Raulien N, Quandt D, Meusch U, Rothe K, Schubert K, Schöneberg T, Schaefer M, Krügel U, et al. (2012) Extracellular Ca^{2+} is a danger signal activating the NLRP3 inflammasome through G protein-coupled calcium sensing receptors. *Nat Commun* **3**:1329.
- Schepelmann M, Yarova PL, Lopez-Fernandez I, Davies TS, Brennan SC, Edwards PJ, Aggarwal A, Graça J, Rietdorf K, Matchkov V, et al. (2016) The vascular Ca^{2+} -sensing receptor regulates blood vessel tone and blood pressure. *Am J Physiol Cell Physiol* **310**:C193–C204.
- Sheldrick GM (2008) A short history of SHELX. *Acta Crystallogr A* **64**:112–122.
- Sheldrick GM (2015) Crystal structure refinement with SHELXL. *Acta Crystallogr C Struct Chem* **71**:3–8.
- Slater J (2016) blindanalysis: v1.0. URL: <http://doi.org/10.5281/zenodo.44678>
- Sterk PJ and Bel EH (1989) Bronchial hyperresponsiveness: the need for a distinction between hypersensitivity and excessive airway narrowing. *Eur Respir J* **2**: 267–274.
- Vogt FG, Williams GR, Strohmeier M, Johnson MN, and Copley RCB (2014) Solid-state NMR analysis of a complex crystalline phase of ronacaleret hydrochloride. *J Phys Chem B* **118**:10266–10284.
- Walsh GM (2017) Biologics for asthma and allergy. *Curr Opin Otolaryngol Head Neck Surg* **25**:231–234.
- Ward DT, Mughal MZ, Ranieri M, Dvorak-Ewell MM, Valenti G, and Riccardi D (2013) Molecular and clinical analysis of a neonatal severe hyperparathyroidism case caused by a stop mutation in the calcium-sensing receptor extracellular domain representing in effect a human 'knockout'. *Eur J Endocrinol* **169**:K1–K7.
- Widler L (2011) Calcilytics: antagonists of the calcium-sensing receptor for the treatment of osteoporosis. *Future Med Chem* **3**:535–547.
- Yarova PL, Stewart AL, Sathish V, Britt RD Jr, Thompson MA, P Lowe AP, Freeman M, Aravamudan B, Kita H, Brennan SC, et al. (2015) Calcium-sensing receptor antagonists abrogate airway hyperresponsiveness and inflammation in allergic asthma. *Sci Transl Med* **7**:284ra60.
- Ye Q, He X-O, and D'Urzo A (2017) A review on the safety and efficacy of inhaled corticosteroids in the management of asthma. *Pulm Ther* **3**:1–18.

Address correspondence to: Daniela Riccardi, School of Biosciences, Cardiff University, The Sir Martin Evans Bldg., Museum Ave., CF10 3AX, Cardiff, UK. E-mail: riccardi@cardiff.ac.uk